



Precipitation of nano-magnesium hydroxide from bittern using ultrasound irradiation

Sh. El Raffie and M. S. Mohamed

National Research Center, Chemical Engineering Department, Cairo, Egypt

ABSTRACT

Fiber and platelet-like Nano-sized $Mg(OH)_2$ particles were synthesized by precipitation of Magnesium rich Bittern 73 g/L Mg^{2+} and ammonia water as precipitator. The influence of aging process on $Mg(OH)_2$ suspension was investigated. The aid of ultrasonic irradiation was studied via synthesis of $Mg(OH)_2$ one-step precipitation reaction. The morphology and properties of the product was analyzed by X-ray diffraction, scanning electron microscope SEM, Fourier transform infrared spectroscopy FT-IR. Thermal analysis TGA –TDA assisted the high decomposition of $Mg(OH)_2$ which can be used as green flame retardant filler. The results showed $Mg(OH)_2$ particles with fiber-like morphology and platelet morphology were obtained with ammonium as precipitator and product was intensively modified by aging process and/or ultrasound waves which increased the surface area and decreased the particle size of $Mg(OH)_2$. Moreover Ultrasound irradiation demonstrated to be a simple and fast method to assist preparation of high crystalline $Mg(OH)_2$. The Nano-crystals size was verified with Transmittance electron microscope TEM. The high resolution electron microscope verified the morphology of the Nano-crystal powder.

Key words: Magnesium hydroxide, Nano- particles, Bittern, chemical precipitation, ultrasound.

INTRODUCTION

Magnesium hydroxide, a very popular environmental, friendly and thermally stable flame-retardant filler in composite materials [1-5] is also used to neutralize acidic waste streams and gases rich in sulfuric oxides [6], as anti-acid excipient in pharmaceuticals [7] in pulp and paper industry [8] as fertilizer additive, and/or the most important precursor for magnesium oxide. In recent years, due to the problems of the increasing number of fine disasters as well as pollution caused by plastic incineration and the appearance of Dioxin, more and more attention has been paid to the environmental protection [9]. Magnesium hydroxide, as non-important kind of inorganic material is a kind of inorganic flame retardant additive advantages contrasted with other flame retardants (i.e aluminum hydroxide), $Mg(OH)_2$ has high decomposition temperature, good effects on depressing smoke and neutralizing acid [10-11]. Scientists all over the world are now showing great enthusiasm on the magnesium hydroxide flame retardant which is bound to have an optimistic market prospect [12-17]. According to the raw material used, the magnesium hydroxide preparation techniques can be mainly defined, into magnesite calcination hydration method, bischofite pyrolysis method, sea water (brine-bittern) line cream magnesium-deposition method, etc.[18]. But, the platelet shape and superfine magnesium hydroxide sample was prepared through ammonia magnesium-deposition method [19-20].

However, most of these approaches are costly, time-consuming and difficult to control the morphology of $Mg(OH)_2$ at room temperature, Ultrasonic irradiation can generate microbubbles in liquid, the cavitation collapses of which produce extremely high temperature (~5000K), pressure (~1000 atm.), heating and cooling rate (> 10-9 K/s), liquid jet streams (~400 km/h), and intense shock waves [21-22]. Previous studies [23-25] indicated that extreme chemical and physical environment was helpful to increase the rate of synthetic reactions and to obtain smaller

crystals with more uniform size distribution compared to the conventional techniques for synthesizing the Nano-cellematerials. Recently, An et al. [26] reported that Nano-sized $Mg(OH)_2$ was sono-chemically synthesized in aqueous phase, and Zhang et al., [27] successfully surface modified micro $Mg(OH)_2$ by using ultrasonic irradiation in an aqueous phase. However, ultrasonic-assisted synthesis and modification of $Mg(OH)_2$ Nano-particles in one-step precipitation.

In this study the high concentrated Bittern was pretreated for purification before preparation of Nano-platelet shape and superfine magnesium hydroxide samples. A comparative ultrasonic assisted synthesis was studied to improve precipitation through ammonia magnesium-deposition.

MATERIALS AND METHODS

2.1 Raw materials

The composition of the main elements in Liquid bittern from Alexandria salt company as the Mg^{2+} raw material is listed in table (1). 25% ammonia water, sodium sulphate, and absolute ethanol were used as analytical grade materials. 10% of (mass fraction) complex solution of gelatin, lauryl sodium sulphate was used as dispersant agent [28].

Table (1) Composition of main elements in Liquid bittern (g/l):

Mg^{2+}	Ca^{2+}	Na^+	K^+	Li^+	Cl^-
73.84	1.6	0.21	9.81	0.0031	0.218

2.2 Preparation of magnesium hydroxide Nano-powder:

2.2.1. Bittern was pretreated by adding 1.5 times equivalent quantity of sodium sulfate as much as the quantity of Ca^{2+} in bittern, in order to eliminate the influence Ca^{2+} on the precipitation process. After addition the bittern solution was stirred at 50°C. The addition and stirring was repeated several times later, Ca^+ ion was precipitated into $Ca(OH)_2$ precipitation and removed from bittern solution.

2.2.2. 200 ml magnesium salt solution of concentration 73 g/l was introduced to the precipitation process in a three-necked flask in water bath 20°C. 10 ml of absolute ethanol and 8 ml. complex solution of (gelatin and lauryl sodium sulfate) were added into the reactor. 30 ml of 25% ammonia water was injected in the three-necked bottle precipitation process was repeated at different periods of time; (30, 60, 80 and 120 minutes).

2.2.3. The suspension of 60 min reaction time was aged 30 minutes at 50 °C. It is well known that crystal nucleus needs enough energy to overcome its energy barrier. So adopting higher aging temperature after precipitation process is beneficial to supply enough energy for $Mg(OH)_2$ Nano crystal to form perfect crystal nucleus. At the same time, higher aging temperature contributes to the volatilization loss of ammonia and growth of grain size. The influence of aging time on crystalline size of $Mg(OH)_2$ Nano-particles was investigated [29-30].

2.2.4. In a typical experiment, Sample was immersed into an ultrasonic bath at 20°C. The equipment model (Autotune series ultrasonic atomizer 20K Hz to 40K Hz 500 watt – 750 watt Model VCX 130 ATFT). The working parameters of the ultrasonic bath was 35 KH and (15 min. waves, 25 second on and 5 second off). The obtained suspension was allowed stirring 60 min at 1000 r/m continuously. The precipitation was separated from mother liquor by filtration (centrifuge is preferred) and washed using diluted ammonia water (60°C) several times to remove other impure ions, such as Na^+ , K^+ , Cl^- and NH^+ .

2.2.5. The final $Mg(OH)_2$ Nano-powders were obtained after dried at 80°C 24 hour in vacuum oven.

2.2.6. Calcination was performed (at 500°C for 2 hours) for portions of both samples of precipitated within 60 min with and without aging. The crystal morphology was compared by SEM and TGA to study the thermal properties.

2.3. Characterization of Nano-powder:

2.3.1. Phase and crystallographic structure of samples were characterized by XRD, which was recorded by using (XRD-IRIGAKU Rint 2500) using Cu K alpha-radiation)

Scanning electron microscope (SEM: JEOL JSM – T20) equipped with energy dispersive X-ray spectrometry (EDS: JED- 2140) for the micro structural observation and qualitative add quantity were used to observe the morphology of the $Mg(OH)_2$ elemental analysis Nano-powders.

2.3.2 The particle and crystal size was available using the TEM microscope for prepared samples in methanol suspension. The Model is JEM -1230, made in Japan, JEOL Co., energy 120 Kv o Steps, Line Resolution: 0.2 nm with Max. Magn. : 600Kx.

2.3.3. Decomposition behavior of Mg(OH)₂Nano powders (thermal analysis):

The TG-DTA curves of the Mg(OH)₂ sample was recorded by means of Schimadzu DIA- SOH, and TGA-50H. Each powdered sample was heated by 10 °C/min, up to 1000 °C with alpha -Al₂O₃ as a reference material.

RESULTS AND DISCUSSION

3.1. Structural (XRD) analysis of the Nano-Mg(OH)₂:

The crystallography of the magnesium hydroxide was analyzed by X-ray diffraction(XRD) and the influence of particle size with different reaction time is shown in Table (2).

Table (2) Influences of particles & crystal morphology with different reaction time

Experimental No.	Reaction time (min)	Mg(OH) ₂ %yield	Mean particle sized Mg (OH) ₂ /nm	Crystal morphology
1	30	50%	45.56	Needle-like crystals
2	60	50%	106.5	More needle-like and fiber-like crystals
3	60+twice volume of alcohol	89.72 %	43.2	Fiber-like and platelet(pan cake)
4	60 + aging (30 min.)	50%	13 nm – 7 nm	Platelet (pan cake) with good dispersion
5	90	50%	59	Aggregated (pan cake)
6	120	50%	79.47	Aggregated (pan cake)
7	60+15 minus	100%	16 nm – 6 nm	Good crystalloid and good dispersion

Table (2) shows the changes magnesium hydroxide mean particle size at different temperatures. The obtained suspensions at (60 min)reaction time was allowed to age for 30 min at 50°C [31].

3.1.1 From (XRD) Fig (1) to Fig (7) shows the main peaks of Mg(OH)₂ formed. The(SEM) images of the crystal powder is illustrated from image (a) to image (g). Fig (5) corresponds to batch obtained at (60 min) reaction time and aged 30 min of mean particle size 61.2 nm- 13 nm.The (SEM) image (e)illustrates the morphology of good dispersion for crystals obtained.XRD of Fig (6) is another batch obtained at (60 min) reaction time was allowed to ultrasonic bath (15min) during addition of chemical and stirring was continued up to (60 min). The mean particle size 16 nm – 6 nm and Image (g) illustrates themorphology of crystals in uniform and good dispersion.The size of the Nano-Mg(OH)₂ decreased after aging and showed more good distribution with ultrasonic waves process.

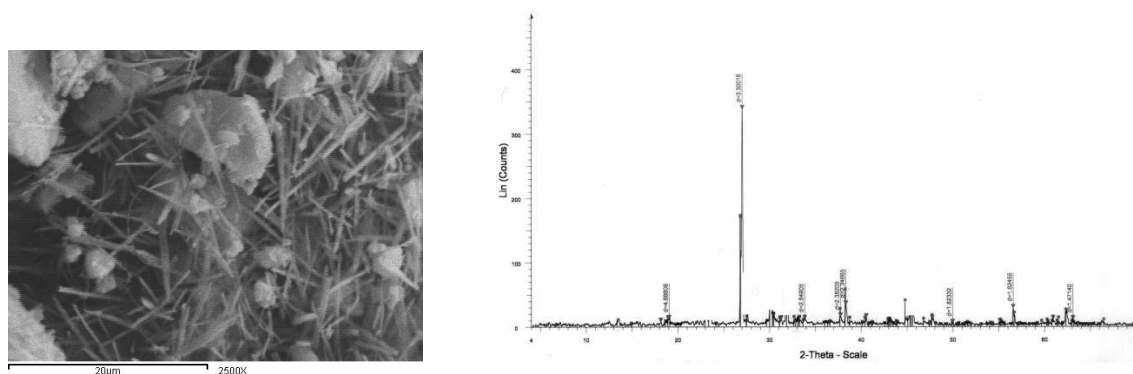


Fig (1) XRD pattern of Mg(OH)₂prepared in30 min reaction Image (a) for Needle-like crystals prepared from 30 min reaction.

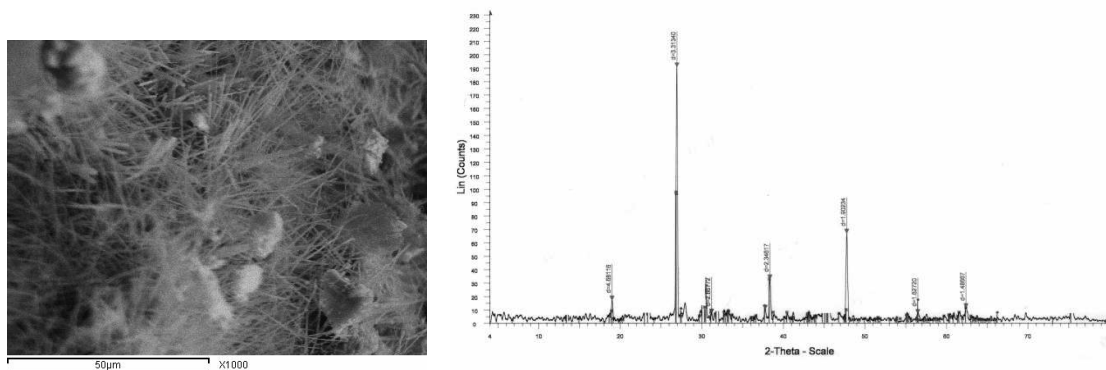


Fig (2) XRD pattern of $Mg(OH)_2$ prepared in 60 min reaction
Image (b) for fiber-like crystals prepared from 60 min reaction.

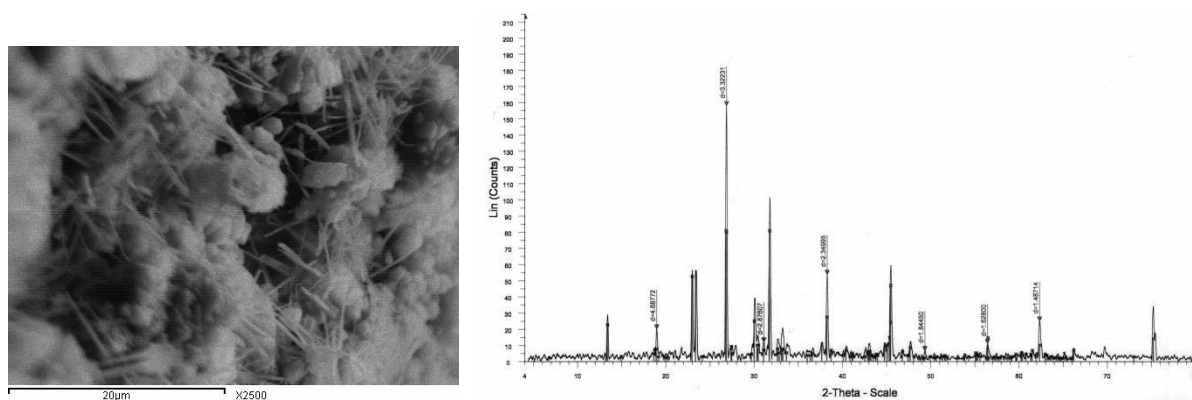


Fig (3) XRD pattern of $Mg(OH)_2$ prepared in 90 min reaction
Image (c) for aggregate of platelet and fiber-like crystals prepared from 90 min reaction.

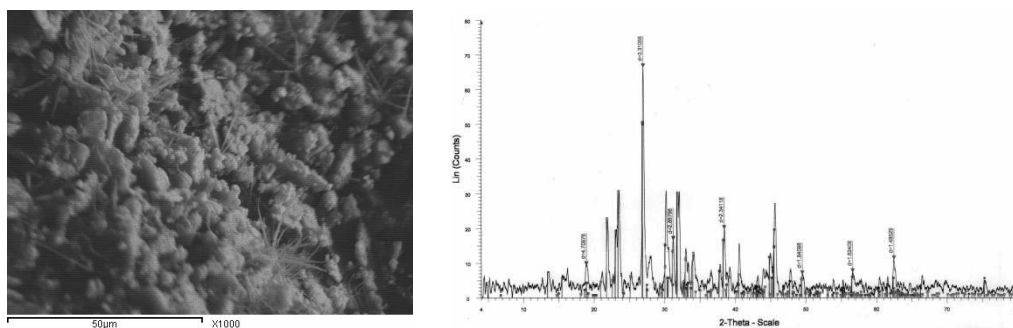


Fig (4) XRD pattern of $Mg(OH)_2$ prepared in 120 min reaction
Image (d) for aggregate of platelet and fiber-like crystals prepared from 120 min reaction.

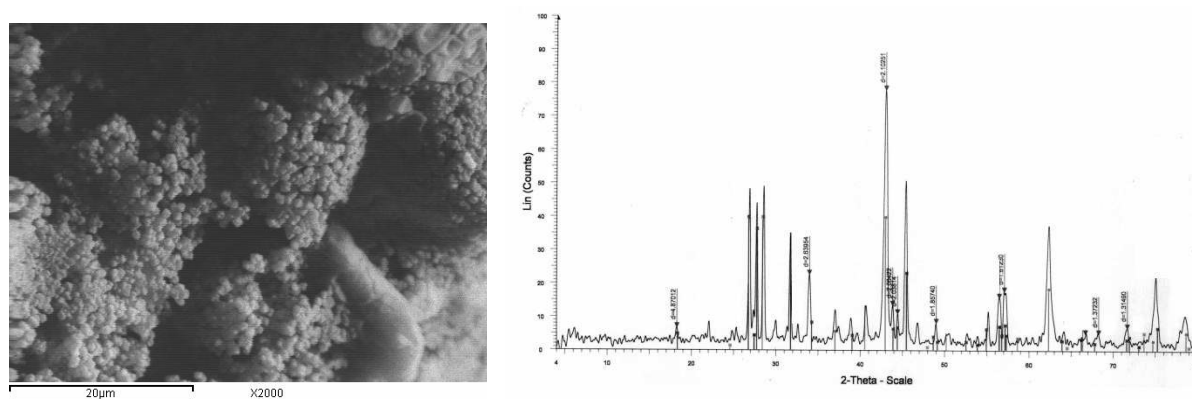
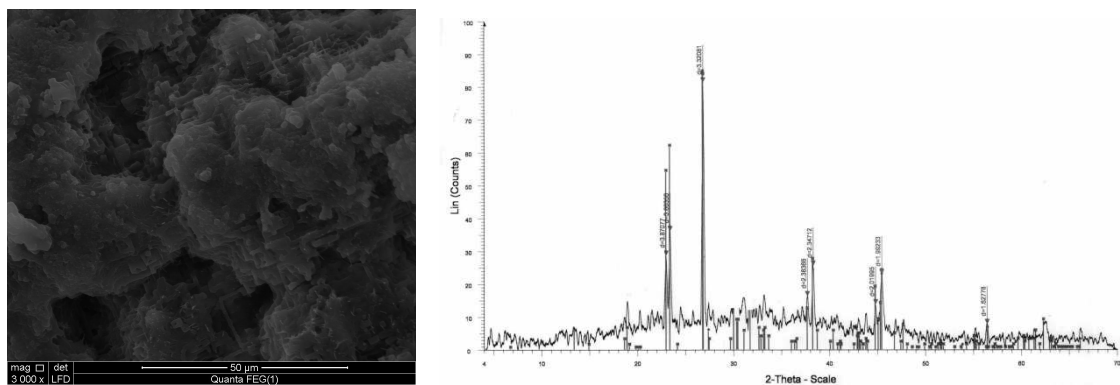


Fig (5) XRD pattern of $Mg(OH)_2$ prepared in 60 min reaction followed by aging 30 min at 50 °C
Image (e) for aggregate of platelet crystals prepared from 60 min reaction followed by aging 30 min at 50 °C.



**Fig (6) XRD pattern of $Mg(OH)_2$ prepared in 60 min reaction with ultrasound 15 min.
Image (f) for aggregate of platelet crystals prepared from 60 min reaction with ultrasound 15 min.**

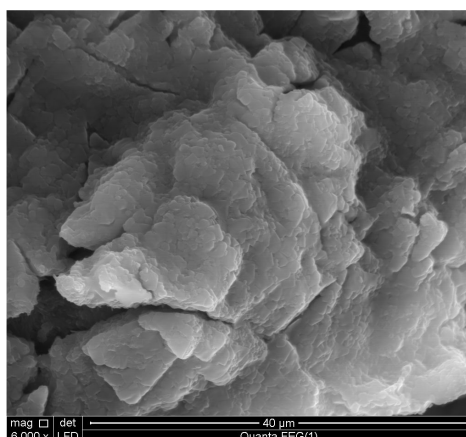


Image (g) for aggregate of platelet crystals prepared from 60 min reaction with ultrasound 15 min

3.1.2 Comparing the obtained (XRD) patterns of suspension obtained at 30(min) Fig (1), 60(min) Fig (2), 90(min) Fig (3) and 120(min) Fig (4) of $Mg(OH)_2$

Fig (1) (XRD) of needle like $Mg(OH)_2$

The peaks at 2θ values of 18.496° , 33.732° , 37.51° , 50.118° and 63.255° corresponds to crystal, size of 32, 52.6, 32.8, 17.4 & 15 of crystalline $Mg(OH)_2$, respectively. The intensity ratio 2.76 exhibits needle-like morphology [32]. In addition the significant broadened peaks indicates that the $Mg(OH)_2$ particles have very small grain size.

Fig(2) XRD of fiber like $Mg(OH)_2$

The peaks at 2θ 18.94° , 31.84° , 38.334° , 47.773° , 56.509° and 62.415° corresponds to the crystal size of 81.3, 195.9, 110.3, 149.6, 129.6, 129.8, and 3.6, of crystalline microstrain $Mg(OH)_2$ respectively, which indicates more fiber-like orientation effect. In addition, the significant broadened peaks indicate more small grain size.

Fig (3) XRD of micro-crystal $Mg(OH)_2$

The peak at 2θ 18.916° , 31.07° , 38.27° , 40.369° , 56.499° and 62.393° , correspond to the crystal size of 43.8, 79.1, 123.2, 3.511, 93.8, and 92.7 of mixed micro strain and Nano-crystalline $Mg(OH)_2$ respectively, which indicates more platelet morphology and some needle type still oriented. The broadened peaks indicated presence of Nano crystals.

Fig (4) XRD of Nano-crystal $Mg(OH)_2$

The peak at 2θ 18.826° , 31.169° , 38.419° , 49.419° , 56.627° and 62.48° corresponds to the crystal size of 27.1, 78.3, 22.8, 64.8, 42.8 and 63.4 of more Nano-crystalline $Mg(OH)_2$ respectively, which indicates the major platelet morphology of Nano crystals and broadened peaks.

3.1.3 Comparing the obtained (XRD) patterns of suspension obtained at 60(min) and more alcohol Fig (I), 60(min) and 30 min aging at $50^\circ C$ Fig (II), 60(min) and ultrasound wave 15 min Fig (III):

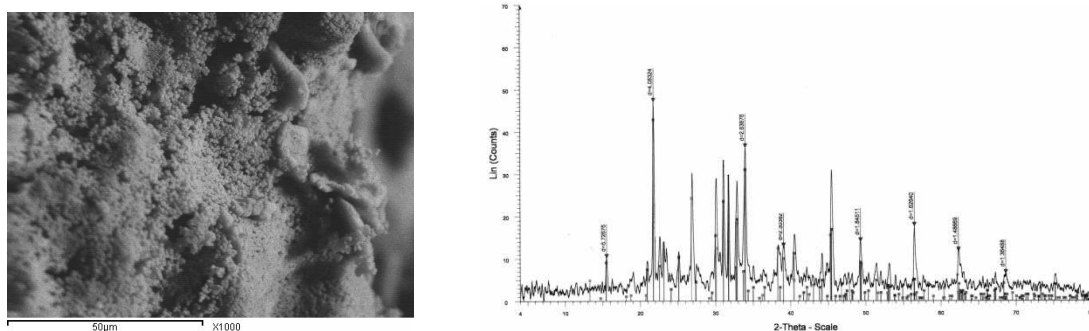


Fig (I) XRD pattern of Mg(OH)₂ yield from reaction time 60(min) with more (OH) groups
Image(f)a illustrate major spread of platelet crystals morphology.

The XRD pattern of Fig (I) corresponds to reaction time 60(min) with more (OH) groups i.e. introducing more alc. (twice volume used before). This reaction increased the yield up to 89.72% Mg(OH)₂ crystalline structure. The powder was then calcined at 500°C 2 hours. The peaks at 2θ 15.46°, 33.972°, 49.352°, 56.539°, 62.414° and 68.717° corresponding to the crystal size of 57.7, 26.2, 90.1, 17.1, 55.8 and 15.5 nanoparticles. The crystal morphology of needle-type for Mg(OH)₂ appears as major spread and the platelet crystals morphology is illustrated too in Image(f)a.

The XRD pattern of Fig (II) corresponds to reaction time 60(min) followed by aging 30 min at 50°C. The powder was then calcined at 500°C 2 hours showing yield 50% Mg(OH)₂ crystalline structure and MgO 50% appeared too. The peak at 2θ 18.201°, 27.675°, 36.996°, 46.77°, 57.079°, and 71.723° corresponding to the crystal size of 45.8, 30.2, 51, 59.9, 46.1, and 39.7 nanoparticles less than 40 nm size. The crystal morphology and EDS is shown in Image(F)b. showing homogenous platelet structure in Nano scale.

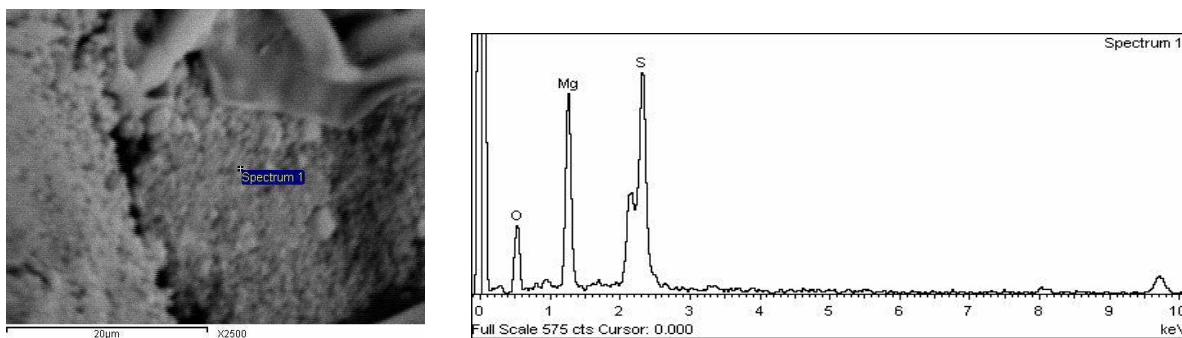


Image (F)b shows crystal morphology and EDS

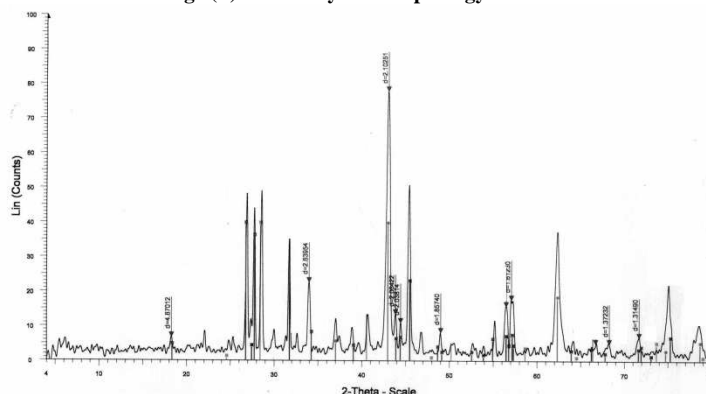


Fig (II) corresponds to reaction time 60(min) with yield 50% Mg(OH)₂ crystalline structure and MgO 50%

The XRD pattern of Fig (III) and image (g) and image (h) corresponds to reaction time 60(min) with good yield 75%- 100% crystalline structure of Mg(OH)₂. The reaction was introduced to ultrasound waves for 15 min during stirring. The peaks 2θ 22.957°, 26.825°, 38.318°, 45.49° and 56.487° corresponding to crystal size of 3,3,3,3 and 167.5 Nano size particles >20 nm. In addition the significant broadened peaks at 26.825° indicated the Nano-particles of Mg(OH)₂ with no additional peaks showing high purity.

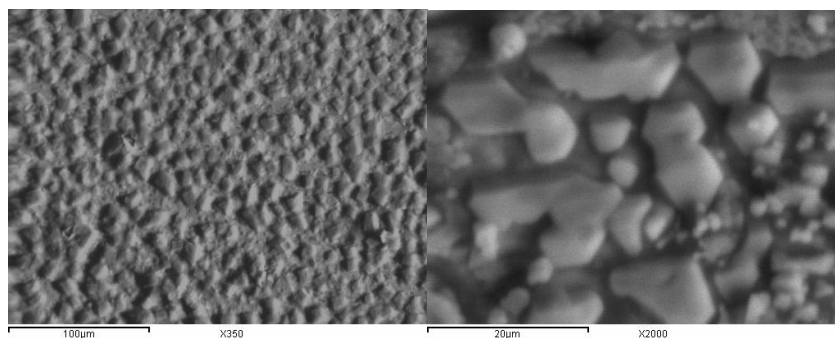


Image (g) SEM of Nano particles of $Mg(OH)_2$ prepared assisted ultrasound waves

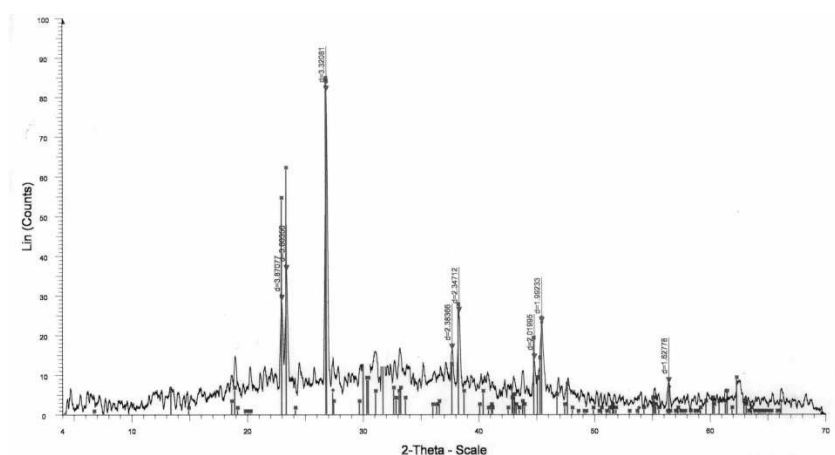


Fig (III) corresponds to reaction time 60(min) assisted with 15 min ultra sound waves

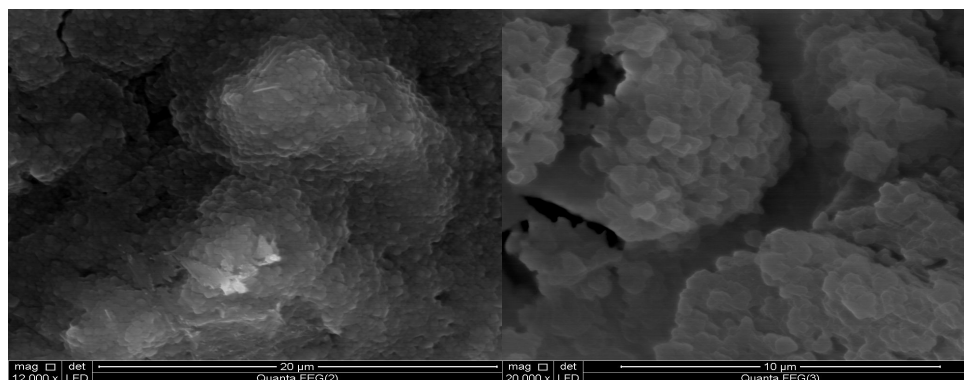
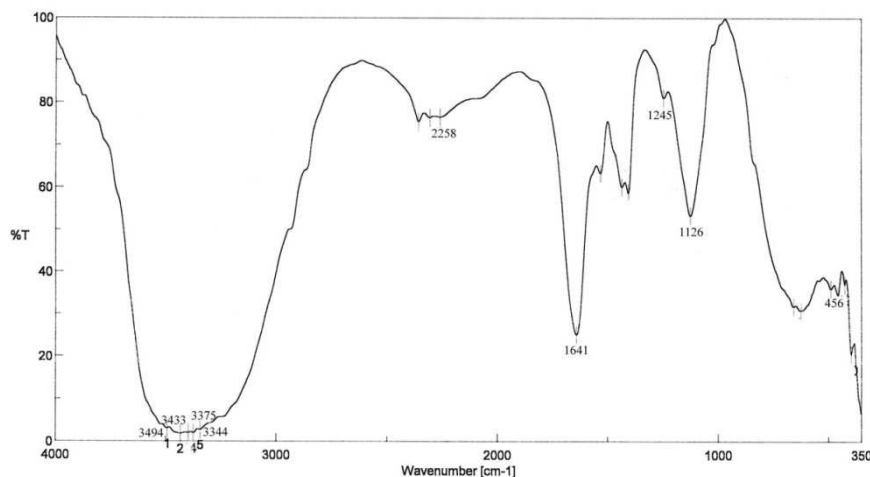


Image (h) Hi- resolution SEM of Nano particles of $Mg(OH)_2$ prepared assisted ultrasound waves

So aging procedure and ultrasound waves are important processes to prepare $Mg(OH)_2$ Nano-particles with perfect crystal. Fig(II) and Fig (III).

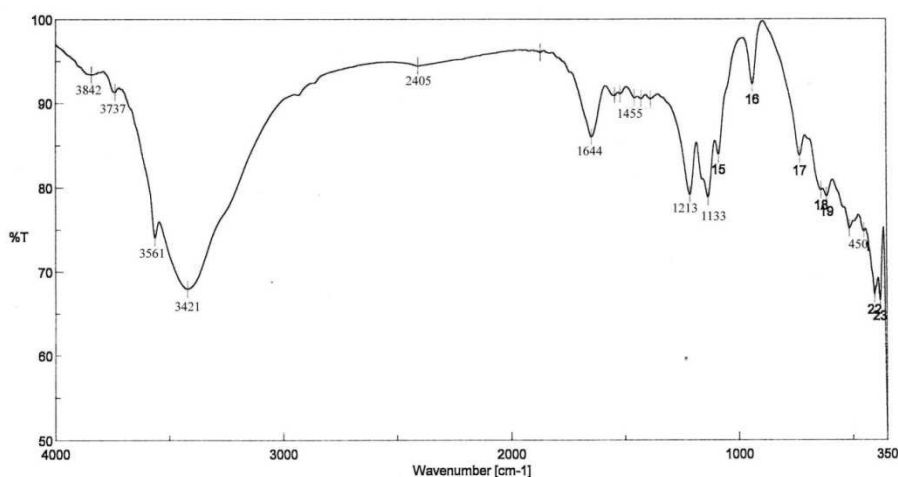
4- FT-IR analysis:

4.1 Fig (5) shows the FT-IR spectrum of the Nano $Mg(OH)_2$ prepared by precipitation process with stirring 120 min. The spectrum shows only intense broad $-OH$ stretching vibration peak at $3494cm^{-1}$, $3433 cm^{-1}$, $3398cm^{-1}$, $3375cm^{-1}$ and $3344cm^{-1}$. The sharp peaks at $1641cm^{-1}$ and $1434cm^{-1}$ confirms the existence of Nano- $Mg(OH)_2$. The peak at $456cm^{-1}$ assigned to $Mg-O$ in $Mg(OH)_2$ crystal structure. The prominent peak observed in Fig (7) at $2900 - 2800 cm^{-1}$, which is mainly due to residual $-OCH_3$ and also due to linearly bound CO_2 . This peaks disappeared in Fig (5) as the for long time preparation process 120 minutes.



Fig(5) FT-IR spectrum of the Nano- $\text{Mg}(\text{OH})_2$ prepared by precipitation process with stirring 60 min.

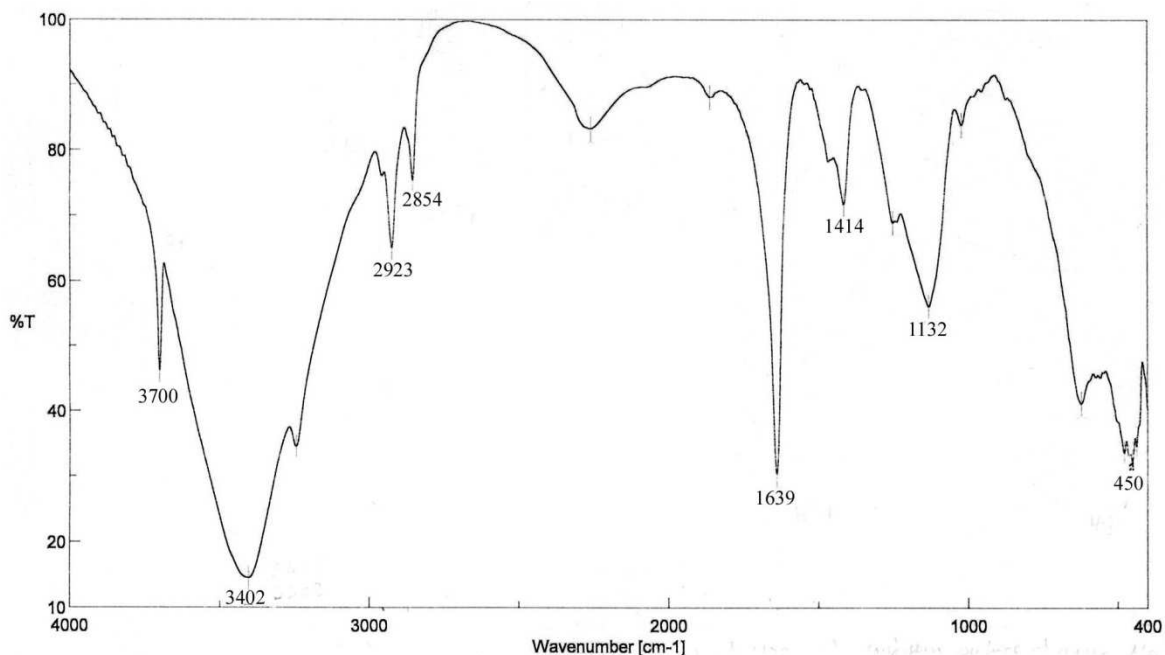
4.2 Fig(6) illustrates the FT-IR spectrum of the Nano- $\text{Mg}(\text{OH})_2$ prepared by precipitation process in 60 min stirring followed by 30 min aging process at 50°C . The dried powder after then was calcined at 500°C for 2 hours. The spectrum is similar to that which is reported in literature [35], with a small peak at 3737 cm^{-1} and intense $-\text{OH}$ stretching vibration peak 3421 cm^{-1} . As can be seen the O-H stretching decreased but still appears as the temperature increased at 500°C . This is because the characteristic of the sample itself is hygroscopic that easily absorbs water molecule when the preparation of sample when characterization process is done [36]. As the temperature was raised, the peaks intensity of O-H stretching bonded with Mg become smaller at temperature 500°C and finally disappears when the temperature reaches above 600°C .



Fig(6) FT-IR spectrum of the Nano- $\text{Mg}(\text{OH})_2$ prepared by precipitation process with stirring 60 min followed by aging 30 min and calcined at 500°C .

Another prominent peak observed at $2900 - 2800\text{ cm}^{-1}$ shown in Fig (7) which is mainly due to residual $-\text{OCH}_3$ but could also partly due to linearly bound CO_2 . This peaks disappeared in Fig (6) as the temperature increased up to 500°C during calcination [37]. The peak at 1644 cm^{-1} and 1455 cm^{-1} are attributed to Mg $-\text{OH}$ and OH bond bending vibration, respectively. The weak peak at 1133 cm^{-1} also confirms the existence of Nano Mg $(\text{OH})_2$. The peak at 450 cm^{-1} assigned to Mg-O in Mg $(\text{OH})_2$ crystal structure.

4.3 Fig(7) illustrates the FT-IR spectrum of the Nano- $\text{Mg}(\text{OH})_2$ prepared by precipitation process with stirring 60 min and sonication 15 min. The spectrum is reported in literature [33] and [34], with a sharp and intense-OH stretching vibration peaks at 3700 cm^{-1} and 3402 cm^{-1} . The peaks at 1639 cm^{-1} and 1414 cm^{-1} are attributed to the Mg-OH and OH bond bending vibration, respectively. The small peaks at 2923 cm^{-1} and 2854 cm^{-1} corresponds to the symmetric and stretching vibrations aliphatic groups $(-\text{CH}_2-)_n$ respectively. The weak peak at 1132 cm^{-1} also confirms the existence of Nano- $\text{Mg}(\text{OH})_2$. The peak at 450 cm^{-1} assigned to Mg-O in Mg $(\text{OH})_2$ crystal structure.



Fig(7) FT-IR spectrum of the Nano- $Mg(OH)_2$ prepared by precipitation process with stirring 60 min and sonication 15 min

5. The Thermal Stability Analysis TG-TDA

5.1 The $Mg(OH)_2$ Nano-powder has high decomposition temperature and is a nontoxic and smoke suppressing. TG-TDA curve of $Mg(OH)_2$ prepared at 60 min with stirring. The TDA curves Fig (8) shows the decomposition of $Mg(OH)_2$ which exhibit a pronounced weight loss in two steps within the temperature range $208^\circ C - 412^\circ C$ with a total percentage of weight loss of -44.655% which can be attributed to the decomposition of $Mg(OH)_2$, accompanied by an endothermic effect. The third step in weight loss of -21.458% in TG profile from temperature range $470^\circ C - 661^\circ C$ corresponds to complete dehydroxylation of brucite according to the following reaction $Mg(OH)_2 \rightarrow MgO + H_2O$.

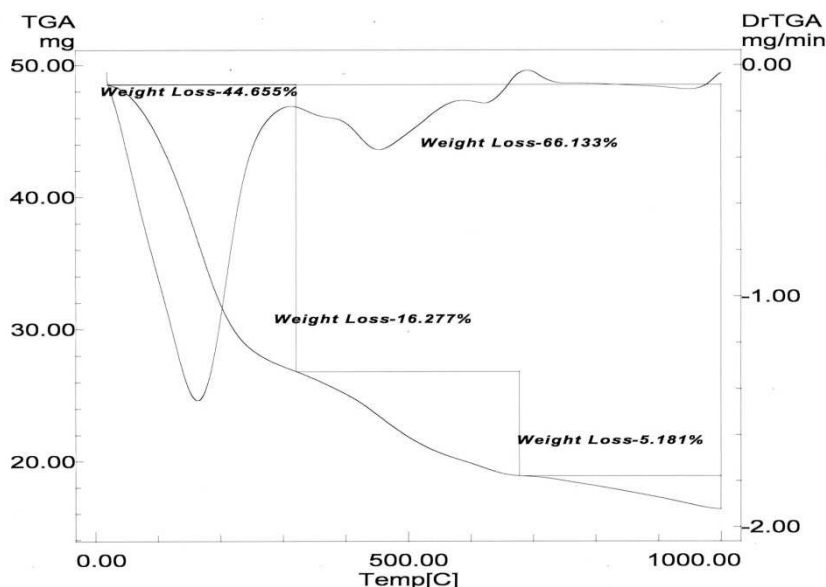


Fig (8) TG-TDA curve of $Mg(OH)_2$ prepared at 60 min

5.2 The TG-TDA curve of $Mg(OH)_2$ prepared at 60 min and aged 30 min at $50^\circ C$ after precipitation reaction, shown in Fig (9). The decomposition behavior of $Mg(OH)_2$ shows a most significant weight loss which is observed at the temperature $464^\circ C$ corresponding to decomposition of $Mg(OH)_2$ to MgO . The mass loss -17.297% from $464^\circ C$ up to temperature $658^\circ C$ indicated the decomposition of intermediate structures of random nuclei production of new phase.

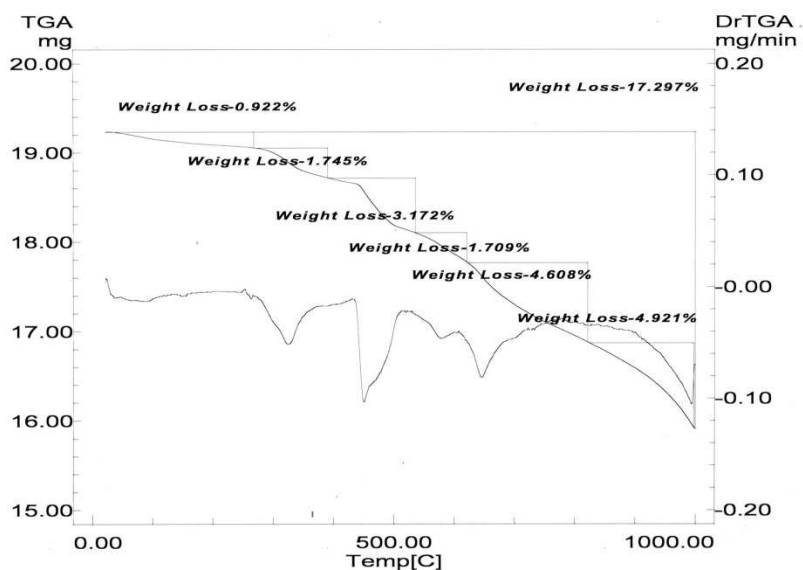
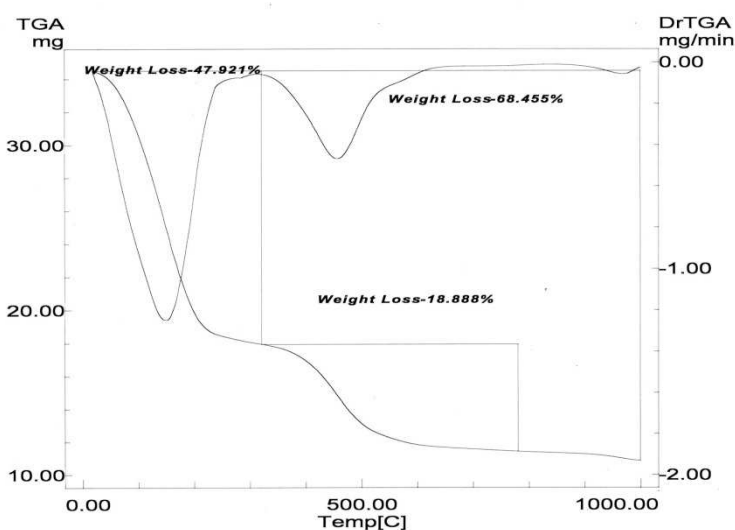


Fig (9) TG-TDA curve of $\text{Mg}(\text{OH})_2$ prepared at 60 min and aged 30 min at 50°C followed by calcination 2 h at 500°C

5.3 TG-TDA curve was performed to investigate the thermal stability of Nano- $\text{Mg}(\text{OH})_2$ as shown in Fig(10). The TDA curve in Fig(10) shows the decomposition behavior of the $\text{Mg}(\text{OH})_2$ sample sono- assisted during precipitation. The decomposition of $\text{Mg}(\text{OH})_2$ sample is predicted to loss of water and crystal water below 310°C . A significant weight loss of -47.9% is observed in the temperature range of $120 - 270^\circ\text{C}$ corresponding to decomposition of $\text{Mg}(\text{OH})_2$ to MgO [30]. The mass loss -68.455% of the sample is reached at temperature 489°C . Over 31% of the reaction of $\text{Mg}(\text{OH})_2$ to MgO from temperature $470^\circ\text{C} - 661^\circ\text{C}$ corresponds to complete dehydroxylation of brucite according to the following reaction: $(\text{Mg}(\text{OH})_2 \rightarrow \text{MgO} + \text{H}_2\text{O})$ indicates that the decomposition process have mostly ended [36].



Fig(10) TG-TDA Curve for decomposition behavior of the $\text{Mg}(\text{OH})_2$ sample sono- assisted during precipitation.

The total % weight loss of Sample prepared at 60 min reaction shown at Fig (8), aged sample for 30 min after preparation shown at Fig (9) and prepared sample assisted with ultrasound waves shown in Fig shown at Fig(10) are -17.297%, -66.133% and -68.455% respectively. It can be noted that the temperature of ultrasonic assisted and sample prepared at 60 min shows much higher total percentage mass loss than that mass loss of aged sample 30 min followed by calcination 2 hours at 500°C . The total percentage mass loss of -17.297 % may be attributed to incomplete decomposition of water bonded molecules from the surface of smaller particle size of $\text{Mg}(\text{OH})_2$ during calcination process to MgO .

6. TEM crystal size analysis:

6.1 Fig (11) a, b, and c shows a typical TEM image of the prepared MgO (aged and calcined). As expected the needle like crystals appeared in the Fig (11) a and Fig (11) b with crystal sizes ranging between 123 and 492 nm.

The Nano- particles with platelets morphology appeared with Nano- size of about 13 nm -7nm in Fig (11) c. Although the aging process helped in the appearance of more platlete like crystals in Nano-size scale but also it did not destroy all needle like crystals which appeared too.

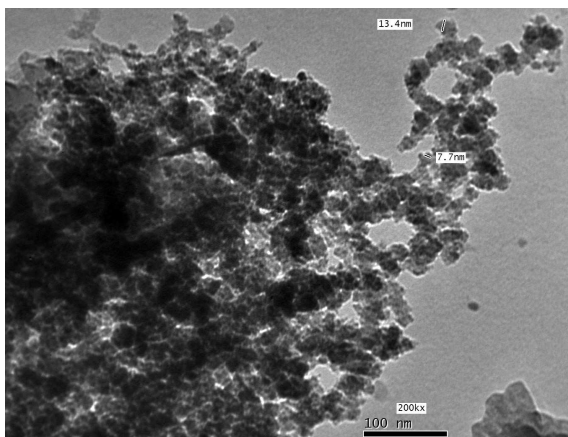
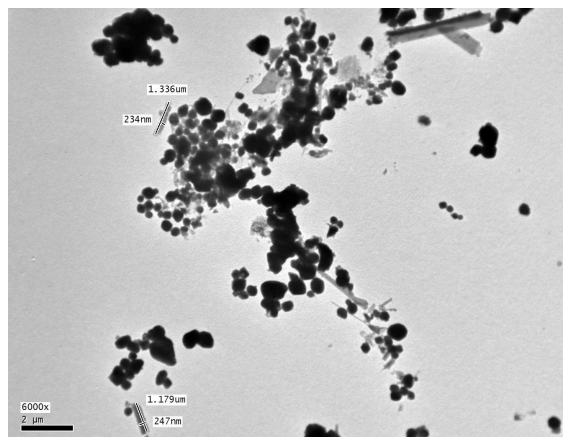
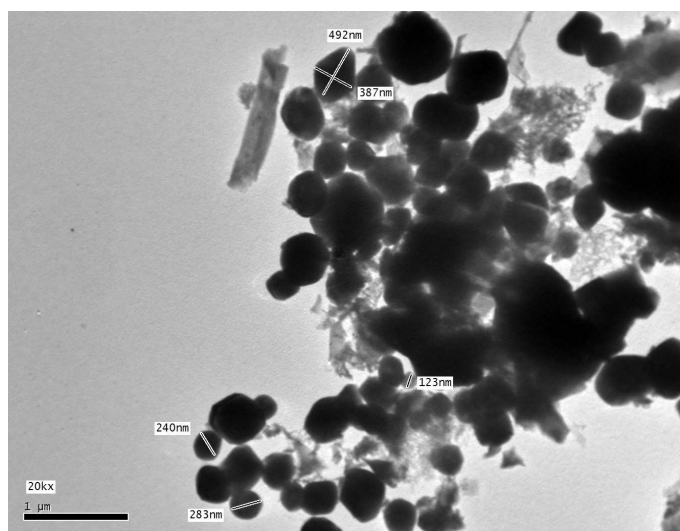


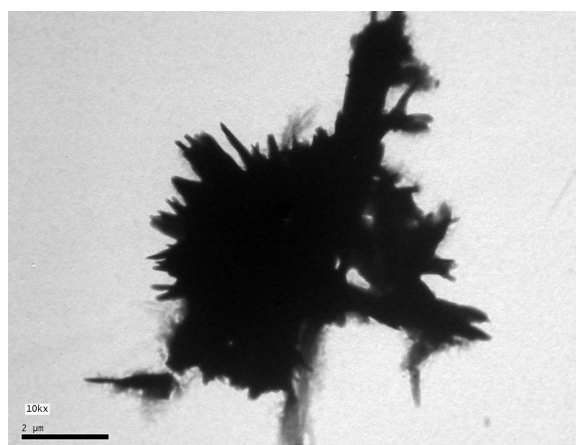
Fig (11)a



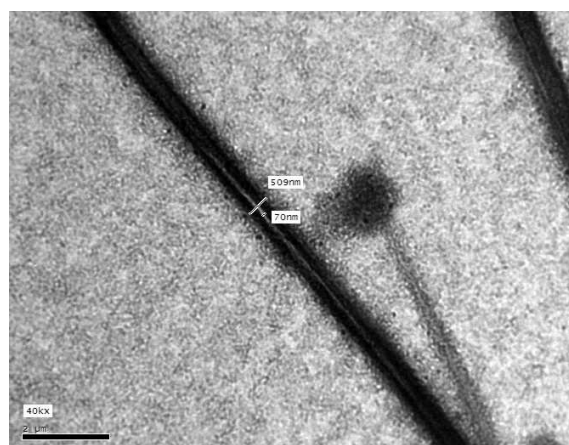
Fig(11) b



Fig(11)c



Fig(12) a



Fig(12)b

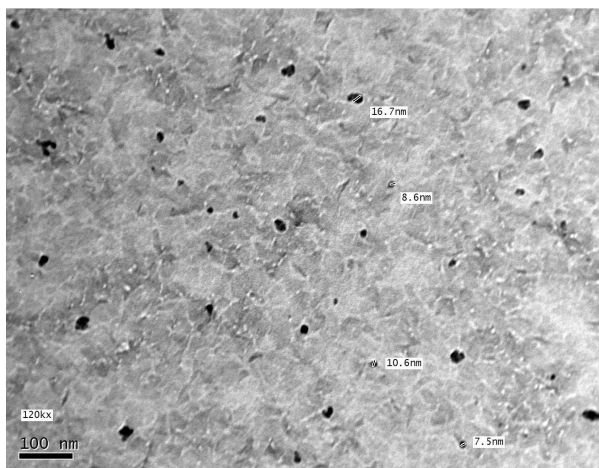


Fig (12)c

Fig (12) TEM image of US precipitated $Mg(OH)_2$ using Ammonia and Bittern

Fig. (11) TEM image of calcined Mg Oat $500^\circ C$ after precipitation using ammonia and bittern and aging 30 minutes. Fig (12) a, b, and c shows the TEM image of $Mg(OH)_2$ prepared using ultrasound irradiation. The platelet aggregates appeared in Fig(12) a in chips morphology as shown before in the high resolution microscope. Fig (12) c shows higher dispersion for the aggregates and platelet crystals with crystal sizes ranging 16nm – 6 nm. It is evident that the average particle size prepared by sonochemical method is much smaller than that prepared by conventional method.

CONCLUSION

Bittern bischofite is selected as low cost raw material while ammonia was selected as the precipitator. However, the conventional precipitation method under magnetic stirring produced $Mg(OH)_2$ having relatively large particle size, along with a requirement of long aging time up to 120 min.

The introduction of aging process at $50^\circ C$ for 30 min overcome problem of large particle size and long aging time 120 min down to 60 min. The results of SEM analysis showed good dispersion of platelet (pan cake) shaped $Mg(OH)_2$ powder.

The ultrasonic irradiation was demonstrated to be a simple and fast method to assist the preparation of high crystalline $Mg(OH)_2$. The Ultrasound irradiation increased specific surface area and decreased the size of $Mg(OH)_2$ illustrated by the high resolution electron microscope.

The TEM analysis results show that the product has a mean granularity of 6 nm- 16 nm, and it is platelet crystal shaped. The ultrasound irradiation yields product with much smaller crystal size which is favorable to dispersibility and adsorption ability.

From the $Mg(OH)_2$ thermal decomposition at $300^\circ C$ - $350^\circ C$ corresponds to chemical reaction represents a system of random nucleation on a large number of small crystallites. At $400^\circ C$ - $450^\circ C$ and $500^\circ C$ corresponds to nucleus production and development. At both temperatures the whole decomposition process is too fast.

Acknowledgement

The Authors gratefully acknowledge the continuous supports from the National Research Center and helpful colleges in the Chemical Engineering Department.

REFERENCES

- [1] Hornsby P.R., Wang J., Rothern R., Jackson G., Wilkinson G., *Polym. Degrad. Stab.*, **1996**, 51, 235.
- [2] Hornsby P.R., Watson G.L., *Plast. Rubber Process. Appl.*, **1989**, 11, 45.
- [3] Pal G., Macskay H. (Eds.), *Plastics their behavior in Fires*, Elsevier, Amstrdam, **1991**.
- [4] Sain M., Dark S.H., Suhara F., Law S., *Polym. Degrad. Stab.*, **2004**, 83, 263.
- [5] Rashmi M. M., Kiran P. and Anuradar V., *Advances in Applied Science Research*, **2012**, 3, 5 2553 – 2560.
- [6] Booster J.L., Van A. S., Reuter M.A., *Miner. Eng.*, **2003**, 16, 273.
- [7] Kang J., Schwendeman P., *Biomaterials*, **2002**, 23, 239.

- [8] kale R.D. and Chet R. M., *Advances in Applied Science Research*, **2012**, 3, 5, 3073-3080.
- [9] Hui XU., Deng X., *Trnsactions of Nano ferrous Metals Society of China*, **2006**, 16, 488-492.
- [10] Bao-giang XU, Dengaua, Yong-nian Dai, Yang B., *Transaction of Nano ferrous Metals Society of China*, **2007**, 17, s671-s674.
- [11] Govind Y. R., Sadananda A. C. and Narender S. R., *Advances in Applied Science Research*, **2012**, 3, 5, 2636-2642.
- [12] Taicm L., *Materials and Design*, **2001**, 22, 1, 15-19.
- [13] Sain M, Park SH, Sahara F., *Polymer Degradation and Stability*, **2004**, 83, 2, 363-367.
- [14] Ranjit KT, Klabudek J, *Chemistry of Materials*, **2005**, 17, 1, 65-73.
- [15] Kozłowski R, Władysław – Prazyblak M, Garc2yk J, *Molecular crystal and liquid crystal Science and Technology, Section A; Molecular Crystals and Liquid Crystals*, **2000**, 354, 195 – 206.
- [16] Cusack P.A, Cross MS, Hornsby PR. *Polymer Degradation and stability*, **2003**, 79, 2, 309 – 318.
- [17] Shikawa T, Maki I, Koshizuka T, et al. *Journal of the Society Materials Science*, **2004**, 53 12, 1301-1308.
- [18] Suman T., Maheshwar Sh., Maldas N.N., Jayashri Sh. and Madhuri Sh. *Advances in Applied Science Research*, **2012**, 3, 5, 2733-2738.
- [19] Krushna C. P. and Nayak P.L., *Advances in Applied Science Research*, **2012**, 3, 5, 3045 – 3052.
- [20] LU JP, Quliz, QU BJ. *Journal of Crystal Growth*, **2004**, 267, 3-4, 676-684.
- [21] Suslick K.S., *Sonochemistry, Science*, **1990**, 24, 7, 1439-1445.
- [22] Mason T.J., Lovimer J.P., *Applied sonochemistry*: Wiley-VCH Verlag GmbH, Weinheim, **2002**.
- [23] Tai G., Guo W., *Ultrason. Sonochem.*, **2008**, 15, 350-356.
- [24] Behboudnia M., Khanbarbaec B., *Collids Surf. A Physicochem. Eng. Asp.*, **2006**, 290, 229-232.
- [25] Chasemi S., Mousavi M.F., Shamsiur M., Karami H., *Ultrason. Sonochem.*, **2008**, 15, 448-455.
- [26] An D., Ding X. Z. W., Liu Y., *A Physicochem. Eng. Asp.*, **2010**, 356, 28-31.
- [27] Zhang F. H., Zhang, Z. Su, *Apple. Surf. Sci.*, **2007**, 253, 7393-7397.
- [28] Liang-ping Lu, QIU Long-Zhen, Qu Bao-jun, *Journal of crystal growth*, **2004**, 267-684.
- [29] Bao-qiang Xu, Deng-Hua, Dai Yong-nian Yang Bin, *Transaction of Nano ferrous Metals Society of China*, **2007**, 17 s671 – s674.
- [30] Xu, Hui, Deng Xing – rong, *Trans. Nonferrous Met. Soc. China*, **2006**, 16, 488-492.
- [31] Guolin Song, Sude Ma, Gucyi Tang, Xiawei Wang, *Colloids and Surface A: physicochem. Eng. Aspects*, **2001**, 364, 95-104.
- [32] Pachler G.R., Metlok F., Gremlich H.G., *Merek FT-IR Atlas: a collection of FT-IR spectra*, Weineim, New York, **1988**.
- [33] Haibo Dong, Zhiping Du, Yonghong Zhas, Dapeng Zhou. *Powder Technology*, **2010**, 198, 325-329.
- [34] Qing Chang, Lihua Zhu, Zhihong Luo, Min Lei, Suicheng Zhang, Hequig Tang. *Ultra sonics Sonochemistry*, **2011**, 18, 553- 561.
- [35] Yu J.C., Xu A., Zhang L., Song R., Wu L., *J. Phys. Chem. B*, **2004**, 108, 64.
- [36] Nur Syazeila Samadi, Mohd, Khairulasyraf Anat Mustajab and Abdul Rahim Yacob. *International Journal of Basic & Applied Science IJBAS – IJENS*, **2010**, 10, 2.
- [37] Echterhoff R., Knozinger E., *Surf. Sci.*, **1990**, 230- 237.
- [38] Haljkia I., Neou-Syngnoua P., Kolits D. *Thermochimia Acta*, **1998**, 320, 75-88.